Goal-Directed Pedestrian Prediction

Eike Rehder
Institute for Measurement and Control Systems
Karlsruhe, Germany
eike.rehder@kit.edu

Horst Kloeden
BMW Forschung und Technik GmbH
Munich, Germany
horst.kloeden@bmw.de

Abstract

Recent advances in road safety have lead to a constant decline of injured traffic participants in Europe per year. Still, the number of injured pedestrians remains nearly constant. As a countermeasure, active pedestrian safety is the focus of current research, for which accurate pedestrian prediction is a prerequisite. In this scope, we propose a method for dynamics- and environment-based pedestrian prediction. We introduce the pedestrian's destination as a latent variable and thus convert the prediction problem into a planning problem. The planning is executed based on the current dynamics of the pedestrian. The distribution over the destinations is modeled using a Particle Filter. Experimental results show a significant improvement over existing approaches such as Kalman Filters.

1. Introduction

Recent advances in pedestrian detection provide a solid foundation for active pedestrian safety in automated vehicles. Still, for implementation of such systems the missing component is accurate pedestrian prediction.

In the past, pedestrian prediction has only been studied in limited scope. Most works focus on dynamical models to predict pedestrian motion [8, 7, 10] . However, pedestrians have the ability to switch their state of motion within an instance, making dynamical models unreliable for longer prediction horizons.

Moreover, purely dynamical models disregard the fact that pedestrian motion is mostly driven by some intention or goal. In the context of traffic, usually this is to reach a certain destination within a given time frame. Few studies have addressed this particular problem of intention-driven prediction [18, 9, 2, 3]. These previous works, however, deal with prediction in static environments and thus predefine possible goals.

Apart from the intention, the surrounding poses a second major influence on pedestrian motion. This is apparent for the case where an obstacle blocks a pedestrian's path. While some authors model spatial influence on pedestrian motion, they all execute their prediction in static environments [18, 4] or at least for a static observer [9]. This significantly simplifies the task, as motion patterns in a specific scene can be observed and re-identified. For a moving observer however, this is no option as the scenes will only be observed at the time of prediction.

In this work we estimate a probability distribution over the future positions of a pedestrian by means of path planning techniques. A pedestrian is represented by his state vector X_t which consists of the position (x_t, y_t) and orientation ψ_t at time instance t, $X_t = (x_t, y_t, \psi_t)^\top$. Additionally, a map with information on the environment is available in form of an occupancy grid Θ_t that is recorded on-line.

To represent the pedestrian's intention, we introduce short term destinations X_T as latent variables. This enables us to use planning-based prediction, so that we can estimate the distribution $p(X^T|X^t, X_T, \Theta_t)$ from probabilistic planning.

At later time instances, we make use of the initial prediction to refine our estimate over the destinations. This is achieved by comparison between predicted and observed behavior of the pedestrian.

The main contributions of this work are

- the introduction of destinations as latent variables that are estimated on-line,
- the use of an entirely probabilistic planning-based prediction of arbitrary path distributions under consideration of dynamics
- the use of location features that are observed from the environment on-line.

In the following, we will go through the approach step by step. In Section 2, we give a brief overview over the related work. In Section 3 we introduce the planning based prediction framework. Results of the presented method are evaluated in Section 4 and we conclude the paper in Section 5.

2. Related Work

Pedestrian prediction has received some attention in research, especially in the context of intelligent transportation systems. In this section, we give a brief overview over state of the art prediction methods.

In general, the problem can be separated into two classes, short term prediction with focus on motion within the next second and long term prediction up to tens of seconds.

For short term prediction, Baysian Filters are widely used, in particular the Kalman Filter (KF) [15] and the Particle Filter (PF) [1]. An extension to the standard KF prediction is the use of interacting multiple models [10, 12]. Also Gaussian Process Dynamical Models have been applied with various input features such as scene flow, motion histograms [7] or even body pose [13]. The body pose has also been used for prediction together with decision trees [16]. A special case of short term prediction is the change of a particular variable such as walking versus standing [17] or entering the lane [11]. However, all of these approaches only focus on the dynamical model of the pedestrian and do not take the environment into account. Since a pedestrian can change his dynamics rapidly, these models are only suitable for short term prediction.

In long term prediction, information from previously observed trajectories is used. Ziebart *et al*. use observed trajectories within a room to infer a goal-directed planning policy for human motion as well as goal prior distributions [18]. Kitani *et al*. extend this approach with various environment features [9]. Chen *et al*. predict long term trajectories from trajectory clustering and matching [2, 3]. In [8], longest common subsequences are used to match observed trajectories to trajectories from a database for prediction. Chung *et al*. use observed trajectories to learn specific spacial effects that influence human motion in a known environment [4].

3. Goal-Directed Pedestrian Prediction

In this work we focus on the task of long term pedestrian prediction as the estimation of a probability distribution. Specifically, we are interested in the distribution over the pedestrian's future states $p(X^T|X^t, \Theta_t)$ given past observations X^t and a map Θ_t. We introduce the pedestrian's destination X_T he wishes to reach at time T as a latent variable to improve prediction. The distribution over the destinations is estimated online.

3.1. Distribution Approximation

The distribution over the pedestrian's state $p(X^T|X^t, \Theta_t)$ is approximated using a grid representation. For this, we discretize the space in pedestrian position (x_t, y_t) and pedestrian orientation ψ_t.

The grid representation allows for a parameter-free approximation of arbitrary distributions. This especially accounts for multi-modal path distributions which are much harder to approximate in parameterized models.

For state transitions we make the Markov assumption so that $p(X_{t+1}|X^t) = p(X_{t+1}|X_t)$. For the sake of legibility, we abbreviate $p(X_t|X_{t-1})$ with Φ_t. Let $t = 0$ be the time instance at which the prediction is executed, from tracking we assume to have an estimate of the current position distribution $p(X_0)$.

3.2. Dynamics-based Prediction

Given the representation as explained in 3.1, we are interested in the transition from the distribution of the pedestrian's state at a previous time instance $t-1$ to the distribution at a later time instance t. This transition represents the probability distribution of the pedestrian's motion, represented by

$$X_t = X_{t-1} + u(v_t, \psi_t), \tag{1}$$

where $u(v_t, \psi_t)$ is the vector of motion computed from the pedestrian's speed v_t and orientation ψ_t. In this work, we use the unicycle model for pedestrian's motion, i.e.

$$u(v_t, \psi_t) = (\Delta t v_t \cos\psi_t, \Delta t v_t \sin\psi_t, 0)^\top, \tag{2}$$

where Δt denotes the discrete time interval for which the prediction should be applied.

Since both the pedestrians state and motion are subject to uncertainty, the distribution $p(X_t|X_{t-1})$ is computed from the convolution of the two input distributions

$$p(X_t|X_{t-1}) = p(X_{t-1}) \otimes p(u(v_t, \psi_t)). \tag{3}$$

For this work, we model velocity v_t and orientation ψ_t as independent variables. We assume the velocity to be normally distributed with given mean and variance. The orientation is von-Mises-distributed with given mean and concentration parameter $\kappa_{\Delta\psi}$. Also, we model motion that is not aligned with the pedestrian's orientation as von-Mises-distributed with zero mean and concentration parameter κ_v

$$\begin{aligned} p(\Delta x, \Delta y, \Delta\psi) \propto \quad & \exp\left(-\tfrac{(\Delta x - \Delta t v \cos(\psi))^2}{2{\sigma_v}^2}\right) \\ & \cdot \exp\left(-\tfrac{(\Delta y - \Delta t v \sin(\psi))^2}{2{\sigma_v}^2}\right) \\ & \cdot \exp(\kappa_{\Delta\psi}\cos(\Delta\psi)) \\ & \cdot \exp(\kappa_v \cos(\angle(\Delta y, \Delta x) - \psi)), \end{aligned} \tag{4}$$

where $(\delta x, \delta y, \delta\psi)$ denote the increment of (x, y, ψ) in one time step.

From discretization of (4) to the grid, we obtain a convolution filter mask A. Given the previous distribution grid Φ_{t-1}, we can approximate (3) by

$$\Phi_t \propto A \otimes \Phi_{t-1}. \tag{5}$$

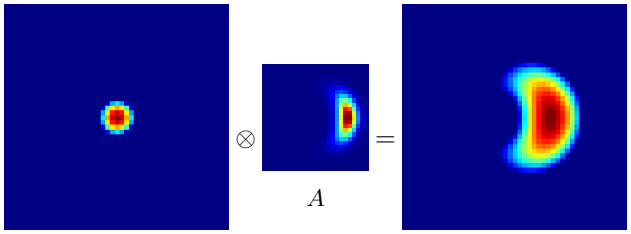

Figure 1: Convolution of an initial distribution with a distribution of motion together and resulting distribution.

The grid Φ_t can be seen as the distribution over the pedestrian's state that he will have reached after t time steps. Due to the relatively small number of non-zero entries in Φ_t and A, the convolution can be computed efficiently using a sparse convolution. For continuous prediction, the convolution (5) can be applied iteratively.

An example for such a convolution is shown in Figure 1. In the first step, the pedestrian's position is normally distributed around the center of the grid while he is assumed to be oriented to the right. Using the motion model from (4) as a filter mask (center), we obtain the right distribution for the following time instance. As it can be seen from the image, the mode of the distribution has shifted to the right while the overall shape is now kidney-like.

3.3. Goal-Directed Prediction

Human actions are usually driven by specific goals. In the case of pedestrian motion this goal is to reach a certain destination within a certain time. We therefore introduce the latent variable of the destination at time instance T, which is now our goal X_T for the planning-based prediction. For now, we assume the distribution over X_T, $p(X_T)$, to be known. We discretize this distribution to obtain the grid Φ_T.

The grid Φ_T is used as an initial distribution for a backward prediction step. For this, we invert the distribution (4) to get the inverse filter mask A^{-1}. We now apply the same scheme as in (5) in backward direction

$$\Phi_{t-1} \propto A^{-1} \otimes \Phi_t. \tag{6}$$

The result of an iterative application of (6) represents the distribution over the pedestrian's state at time instance t so that he will reach the state X_T at time instance T.

In a next step we assume starting state X_0 and goal state X_T to be independent. Under this assumption, a pedestrian's path from X_0 towards X_T can be computed as the multiplication of (5) and (6).

Let Φ_t^+ be the distribution over X_t at time instance t, obtained from forward planning (5) and Φ_t^- accordingly the distribution from the backward prediction (6). We now compute the distribution of the pedestrian's state given his start and goal state with

$$p(X_t|X_0, X_T) \propto \Phi_t^+ \Phi_t^-. \tag{7}$$

This result is crucial as this means that we can apply the forward facing prediction and backward facing prediction iteratively and by multiplication of the results obtain the transition distribution of all intermediate time instances. For uncertain arrival times T, multiple predictions can be obtained from a shift of the backward facing predictions in time dimension. Thus, marginalization over the arrival time is easily implemented.

3.4. Location Prior

Apart from the dynamics and the destination of a pedestrian, the environment also plays an important role in pedestrian motion. One example is an obstacles blocking the direct path towards the destination. Furthermore, a pedestrian will behave differently when walking on the road compared to walking on the sidewalk.

For this reason effects of the environment should also be modeled in the prediction. Given information on the surrounding in form of a map Θ_t, a location prior $p(X_t|\Theta_t)$ is introduced that represents the probability that a pedestrian will enter a certain state given the location of that state. In our prediction framework, this is modeled as

$$\Phi_t^+ \propto p(X_t|\Theta_t)\left(A \otimes \Phi_{t-1}^+\right) \text{ and} \tag{8}$$

$$\Phi_{t-1}^- \propto p(X_t|\Theta_t)\left(A^{-1} \otimes \Phi_t^-\right). \tag{9}$$

In context of the discrete grid, the probability distribution $p(X_t|\Theta_t)$ can be understood as the probability that a pedestrian will enter a certain cell in the grid given its location features, e.g. a pedestrian will less likely enter a cell if it is occupied by another object.

Figure 2 shows the effects of such a prior on the prediction. In this simulative example, four non-traversable objects were introduced (Fig. 2a). If the pedestrian tries to walk from the upper left area towards the lower right, his path will have to avoid the obstacles (Fig. 2b). The distribution over the pedestrians location at one time instance in between the start and end time is depicted in Fig. 2c to visualize the multi-modal outcome of the prediction.

In real situations however, the prior distribution may not be binary only. Instead, multiple cues such as objects, road, sidewalk, etc. may influence a pedestrian's behavior. Thus, we estimate the prior $p(X_t|\Theta_t)$ as a grid according to the discretization of Φ_t. The estimate is applied cell-wise, i.e. we assume the probabilities of all cells to be independent.

For computation, we utilize a grid Θ_t, containing a multitude of features. Let θ_i be a vector of location features of

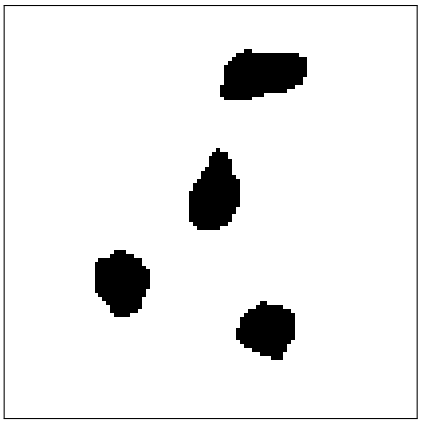

(a) Prior map with four non-traversable obstacles (black).

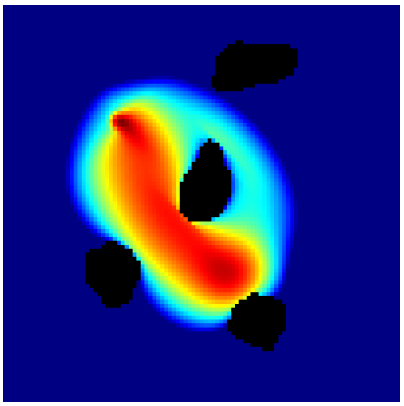

(b) Predicted logarithmic path distribution from top left to bottom right. Blue is low, red high probability.

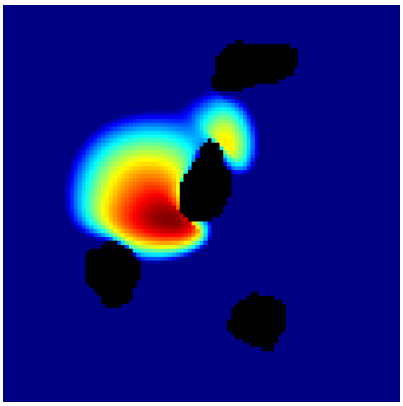

(c) Logarithmic probability distribution of one intermediate time instance. Blue is low, red high probability.

Figure 2: Integration of location information to prediction (simulation results): location prior, logarithmic path distribution and logarithmic distribution prediction for one time instance along the path.

cell i. The prior $p(X|\theta_i)$ is then computed as a single layer perceptron with

$$p(X|\theta_i) = \frac{1}{1+\exp\left(-a^\top \theta_i\right)}, \tag{10}$$

where $a^\top$ represents the weighting parameters for the different features.

To obtain the weights in (10), ground truth pedestrian trajectories are used for supervised learning. For this, a set of N trajectories $(\zeta_1, \ldots, \zeta_N)$ with M individual measurements $\zeta_i = \{X_1, \ldots, X_M\}$ and corresponding grid maps Θ_i is known. We apply the pedestrian prediction according to (7) using (8) and (9) and convert the result into a path distribution to be independent of time effects such as inaccurate velocity estimation.

The path distribution is computed from

$$p(X^M|X_0, X_T, \Theta_t) = 1 - \prod_{\tilde{t}=0}^{M}(1 - p(X_{\tilde{t}}|X_0, X_T, \Theta_t)), \tag{11}$$

so that the result denotes the probability for every cell that it is part of the pedestrians path from X_0 towards X_T, e.g. as depicted in Fig. 2b.

This path distribution is then evaluated on the ground truth trajectory ζ_i. The result is the predicted probability of the pedestrian's actual path. The higher the result, the better the prediction. Thus, to train the weight $a^\top$, we try to maximize this value. Equivalently, we can instead minimize the negative logarithm

$$J(a) = -\sum_{\zeta_i \in} \sum_{X_j \in \zeta_i} \log(p(X = X_j|X_0, X_T, \Theta_t)). \tag{12}$$

The minimum is determined using existing minimization approaches such as gradient descent.

3.5. Goal Distribution Estimation

As mentioned above, the goals X_T have been introduced as latent variables and thus the distribution $p(X_T)$ has to be estimated. In this work, the distribution is modeled as a Gaussian Mixture Model. In order to iteratively improve our mixture $p(X_T)$, the components are represented by a Particle Filter. Every particle represents one mixture component with the location X_T and uncertainty together with the corresponding prediction. The particle weights represent the mixing coefficients. Through the use of multiple mixing components, multiple prediction hypotheses such as crossing or stopping can be represented implicitly.

For initialization, the goals are uniformly distributed around the pedestrian. Then, a prediction is executed according to (7). Once a new measurement of the pedestrian's position is acquired, the prediction can be evaluated against it.

Let $p(X_t)$ be the estimated distribution for the pedestrian's state, obtained by measurement at time instance t. Furthermore, let $p(X_t^-|X_0, X_T, \Theta_t)$ denote the distribution of that state obtained from prediction at a previous time instance. Under the assumption of independence, we can obtain

$$\begin{aligned} &p_{X^-}(X_t^-|X_0, X_T, \Theta_t) \\ &\quad \propto p_{X^-}(X_0, X_T, \Theta_t|X_t^-)p(X_t^-). \end{aligned} \tag{13}$$

If we marginalize over X_t and assume independence of the goal w.r.t. the initial state X_0 and the map Θ_t, we can

(a) Camera image [8]

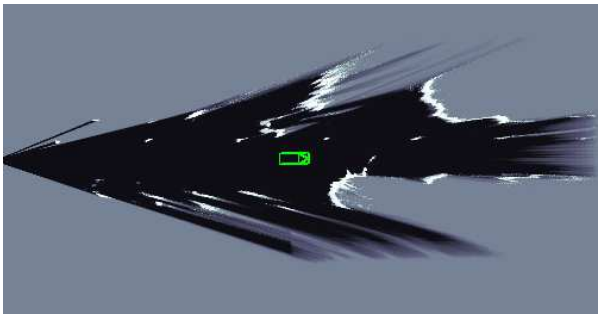

(b) Occupancy grid for obstacles.

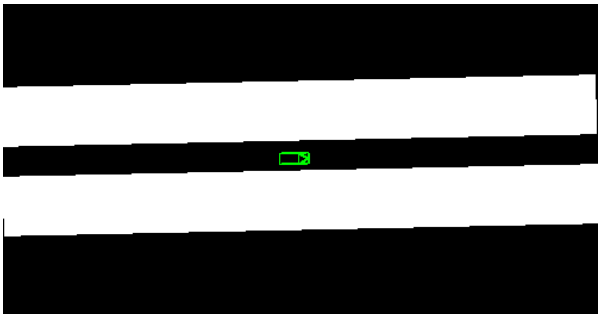

(c) Occupancy grid for sidewalks.

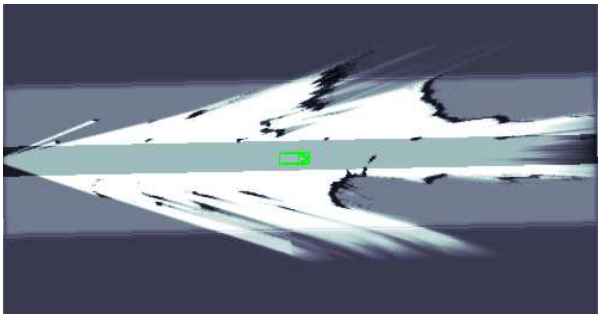

(d) Final location prior distribution map.

Figure 3: Occupancy grids and resulting location prior map. Dark tones encodes low, bright tones high probability.

obtain

$$p(X_T) \propto \int p_{X^-}(X_0, X_T, \Theta_t | X_t) p(X_t) dX_t. \qquad (14)$$

The distribution (14) is now evaluated for the individual particles and the result is used for reweighting. Unlikely particles are discarded and randomly resampled at other locations.

4. Experimental Results

The proposed method is evaluated on the dataset presented in [8]. Pedestrian bounding boxes are taken from the ground truth labels. The pedestrian trajectories are computed from stereo imaging [14] and optimized for outlier rejection.

For the mapping of the environment, we construct standard occupancy grids [5] from disparity images. In addition to this, we make the assumption of a linear road model with predefined width and synthetically compute grid maps for road, sidewalk and curb features without sensor evidence. This assumption holds for most of the sequences but should be replaced by online perception for arbitrary environments.

Both training and test sequences are split into multiple smaller trajectories with a duration of four seconds with maximum overlap of two seconds.

In the training phase, all model parameters, i.e. the motion model (4) and the prior distribution, were optimized by minimization of (12). Location features were a bias term for a uniform prior and features computed from the grid maps mentioned above. These features, apart from the raw maps themselves, were softened versions obtained from Gaussian blur with different variances in order to model preferred distances to objects etc. [18].

As a reference, Figure 3 shows a camera image with corresponding occupancy grid map and sidewalk grid map together with the resulting prior map.

As performance metric we evaluate the predicted probability of the ground truth path. We do not rely on measures such as mean squared distance to the mode or expectancy as this measure does not represent the flexibility of our multimodal approach. The results of all trajectories for all test samples were averaged.

4.1. Path Prediction

In a first step we evaluate the performance of the prediction with given goal states for different environmental features. This is of interest as a better prediction towards the goal will lead to a better estimate of the pedestrian's goal in the later goal inference step.

We train the prior distribution according to (10) with different feature vectors θ_i. The minimization of (12) is ex-

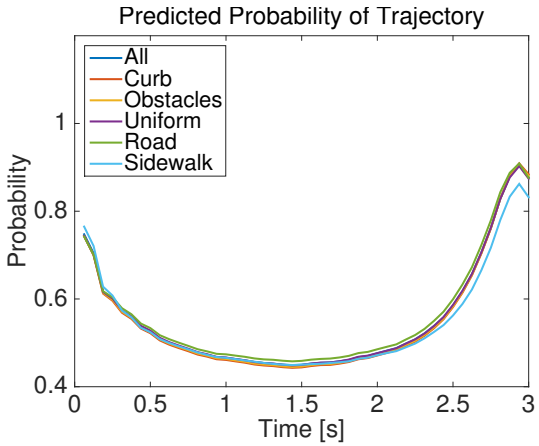

(a) Predicted trajectory distribution evaluated at ground truth trajectory using different location features.

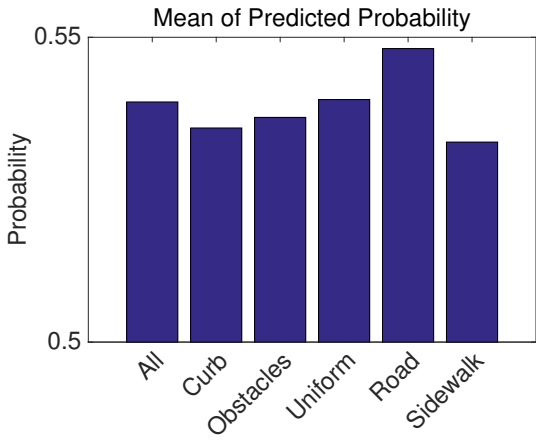

(b) Geometric mean of predicted trajectory probability for different location features.

Figure 4: Evaluation of trajectory prediction using known destinations and different location features.

ecuted for every feature set on the entire training data set. The trained parameters were applied for prediction on the test data set. For both training and testing the start distribution $p(X_0)$ and goal distribution $p(X_T)$ are taken from the ground truth trajectory as normally distributed around start and end point, respectively, with a small variance.

For the results shown in Fig. 4, we evaluated the predicted trajectory with influence of different location features. The features that were used are a uniform prior, i.e. a constant value for all cells, and grid maps, individually containing curb, road, sidewalk and obstacle features [6]. The results show the preformance for all individual features as well as a weighted sum of all possible features. The probability was integrated over a radius of twenty centimeters around the ground truth as this is roughly the space a pedestrian occupies.

The resulting probability of the trajectory at different prediction times is shown in Figure 4a. The results only show small differences for the different location features. This is due to the fact that a known goal has a much larger influence on the prediction. This can also be seen from the hyperbolic shape of the predicted probability. The instantiation of the start and goal state from ground truth already lock the prediction in those two locations.

To get a comprehensible comparison between the prediction results, we computed the geometric mean of the prediction over time. We rely on the geometric mean rather than the arithmetic to penalize low prediction values. The results shown in Fig. 4b show the expected small variation in prediction. Only the use of road features has a noticeable effect. This again can be explained from the known goal state that affects the prediction much more.

4.2. Prediction with Goal Inference

After the evaluation of the pure prediction we also evaluate the prediction with unknown goal states. For this, we use the parameters obtained from training as described in the previous section.

Again we use the subsequences of the test data. Of the four seconds we use one second as observation for the prediction and predict roughly three seconds into the future. As a reference, we added prediction results of a Kalman Filter with a constant velocity model. As we use a constant initialization variance in the starting state for our prediction model, we evaluate this for the Kalman Filter, too. In the following, we refer to the Kalman Filter prediction with the initial state taken from the ground thruth and initialized with the same values as our model as *KF-GT* while the Kalman Filter prediction initialized from Kalman Filter tracking is referred to as *KF-Track*.

Figure 5 shows the results of the prediction with latent goals, evaluated according to 4.1. For the Particle Filter, eight particles were used. Again, the results of the prediction with different location features only feature minor differences, however now larger than in the previous case in 4.1 (see Fig. 5b). Compared to the Kalman Filter initialized from tracking, our prediction model performs slightly worse for the first second. This is mainly due to discretization artifacts that have a stronger influence for short time horizons. The Kalman Filter initialized from the ground truth can even predict with higher relative accuracy during the first 1.5 seconds, as its initial state is directly taken from the ground truth and thus, the velocity estimate is bound to be correct. However, for larger prediction horizons above 1.5 seconds, our prediction clearly outperforms both Kalman

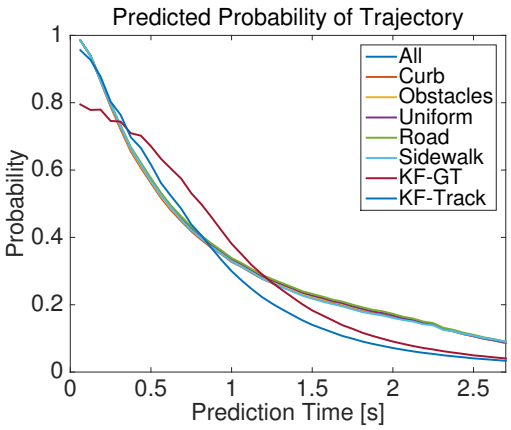

(a) Predicted trajectory distribution evaluated at ground truth trajectory using different location features.

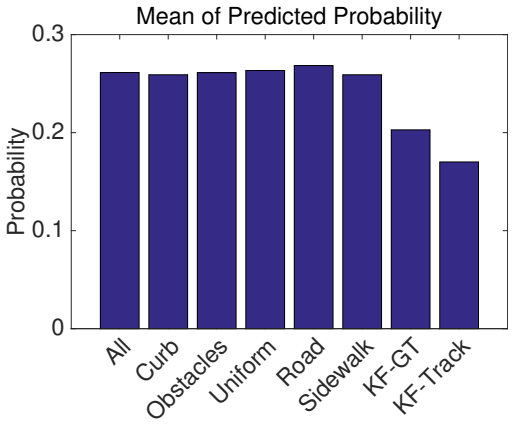

(b) Geometric mean of predicted trajectory probability for different location features.

Figure 5: Evaluation of trajectory prediction using estimation of latent destinations and different location features.

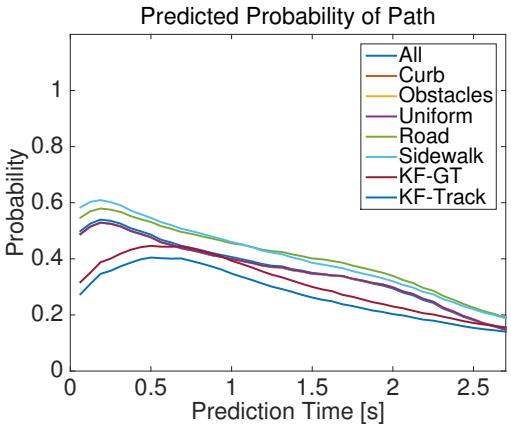

(a) Predicted path distribution evaluated at ground truth trajectory using different location features.

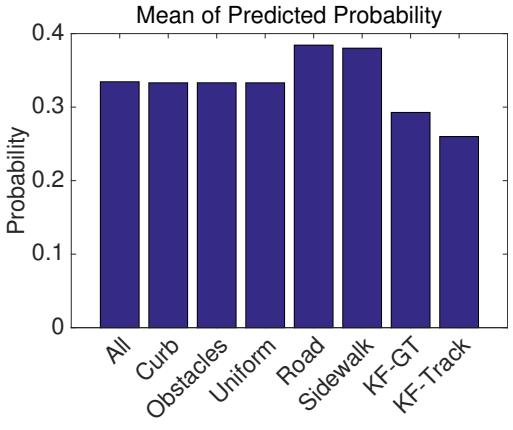

(b) Geometric mean of predicted path probability for different location features.

Figure 6: Evaluation of path prediction using estimation of latent destinations and different location features.

Filter versions.

When evaluating the predicted path of a pedestrian as in (7), the differences become much clearer (Fig. 6). For evaluation, we again integrate over a slightly enlarged area, this time to compute the mean instead of the actual integral. Regarding the prediction of all positions of the pedestrian along the path, this results in slightly underestimated prediction in the first 0.5 seconds as seen in Figure 6a, but overall leads to more robust evaluation. For the path, again, the use of road or sidewalk features result in the best prediction. Also, note that the prediction accuracy drops after about two seconds of prediction time. At this time, the pedestrian will be close to reaching his goal, so the goal location becomes more prominent in prediction. Thus, small miss-estimations in the goal distribution will lead to inaccurate prediction close to the maximum prediction time.

For reference, sample scenes taken from a drive with inner city scenarios are shown in Figure 7. The left column shows camera images taken from a driving vehicle, the right column shows the prior map in desaturated colors together with path predictions. Note the strong influence of the surrounding on the prediction as well as the multiple possible destinations that are estimated for some pedestrians.

(a) Prediction of pedestrian on sidewalk. Possibility of stepping on the street is still tracked in Particle Filter, passing through the fence is excluded from path possibilities.

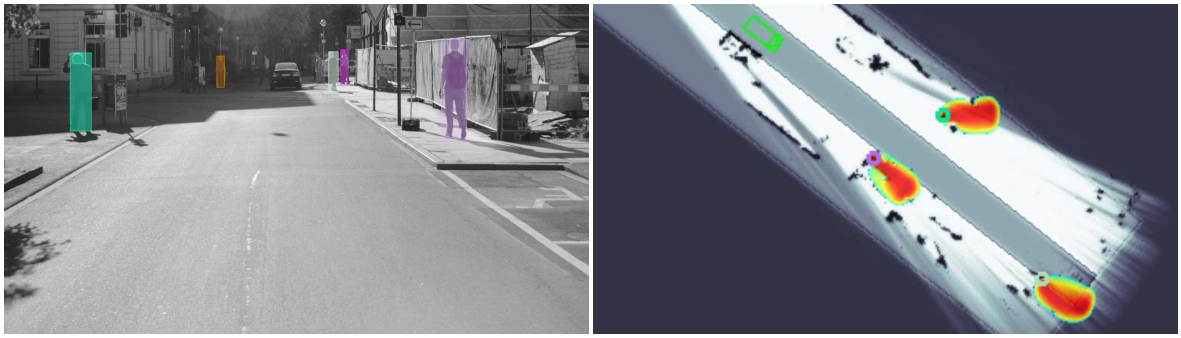

(b) Prediction for multiple pedestrians. Note the exclusion of obstacles in the predicted paths as well as the multiple hypotheses for the most remote pedestrian.

(c) Prediction of pedestrians crossing. Future walking direction on sidewalk is correctly inferred.

Figure 7: Prediction of pedestrians, scenes taken in inner city, manually annotated pedestrians together with their path predictions in context of location prior map. Prior: brighter means higher probability, path: more red encodes higher probability.

5. Conclusion

In this work we presented a method for probabilistic goal-directed pedestrian prediction. By estimation of the pedestrian's destination as a latent variable the prediction problem was converted into a planning problem. Under this assumption the influence of the environment was included in the prediction phase. In contrast to other prediction methods, no model interpretation such as different dynamic states or behavior models is needed, but instead this is solved implicitly.

The modular structure of the model allows for simple addition of other sources of information. Different motion models, such as constant acceleration etc., can be included by modification of the filter masks. Dynamical environments such as passing cars can be modeled using time-varying location priors. The reweighting or resampling step of the goal distribution could also be improved using contextual information.

Overall the prediction already shows a high level of performance with its particular strength in long term prediction.

References

[1] Y. Abramson and B. Steux. Hardware-friendly pedestrian detection and impact prediction. In *Intelligent Vehicles Symposium, 2004 IEEE*, pages 590–595, June 2004.

[2] Z. Chen, D. C. K. Ngai, and N. H. C. Yung. Pedestrian behavior prediction based on motion patterns for vehicle-to-pedestrian collision avoidance. In *Intelligent Transportation Systems, 2008. ITSC 2008. 11th International IEEE Conference on*, pages 316–321, Oct 2008.

[3] Z. Chen and N. H. C. Yung. Improved multi-level pedestrian behavior prediction based on matching with classified motion patterns. In *Intelligent Transportation Systems, 2009. ITSC '09. 12th International IEEE Conference on*, pages 1–6, Oct 2009.

[4] S.-Y. Chung and H.-P. Huang. A mobile robot that understands pedestrian spatial behaviors. In *Intelligent Robots and Systems (IROS), 2010 IEEE/RSJ International Conference on*, pages 5861–5866, Oct 2010.

[5] A. Elfes. Using occupancy grids for mobile robot perception and navigation. *Computer*, 22(6):46–57, June 1989.

[6] H. Harms, E. Rehder, and M. Lauer. Grid map based curb and free space estimation using dense stereo vision. In *Intelligent Vehicles Symposium Proceedings, 2015 IEEE*, June 2015.

[7] C. Keller and D. Gavrila. Will the pedestrian cross? a study on pedestrian path prediction. *Intelligent Transportation Systems, IEEE Transactions on*, 15(2):494–506, April 2014.

[8] C. G. Keller, C. Hermes, and D. M. Gavrila. Will the pedestrian cross? probabilistic path prediction based on learned motion features. In *Pattern Recognition*, pages 386–395. Springer, 2011.

[9] K. M. Kitani, B. D. Ziebart, J. A. Bagnell, and M. Hebert. Activity forecasting. In *Computer Vision–ECCV 2012*, pages 201–214. Springer, 2012.

[10] H. Kloeden, D. Schwarz, R. H. Rasshofer, and E. M. Biebl. Fusion of cooperative localization data with dynamic object information using data communication for preventative vehicle safety applications. *Advances in Radio Science*, 11:67–73, 2013.

[11] S. Kohler, M. Goldhammer, S. Bauer, K. Doll, U. Brunsmann, and K. Dietmayer. Early detection of the pedestrian's intention to cross the street. In *Intelligent Transportation Systems (ITSC), 2012 15th International IEEE Conference on*, pages 1759–1764, Sept 2012.

[12] J. F. P. Kooij, N. Schneider, F. Flohr, and D. M. Gavrila. Context-based pedestrian path prediction. In *Computer Vision–ECCV 2014*, pages 618–633. Springer International Publishing, 2014.

[13] R. Quintero, J. Almeida, D. Llorca, and M. Sotelo. Pedestrian path prediction using body language traits. In *Intelligent Vehicles Symposium Proceedings, 2014 IEEE*, pages 317–323, June 2014.

[14] B. Ranft and T. Strauss. Modeling arbitrarily oriented slanted planes for efficient stereo vision based on block matching. In *Intelligent Transportation Systems (ITSC), 2014 IEEE 17th International Conference on*, pages 1941–1947, Oct 2014.

[15] N. Schneider and D. M. Gavrila. Pedestrian path prediction with recursive bayesian filters: A comparative study. In *Pattern Recognition*, pages 174–183. Springer, 2013.

[16] H. Sidenbladh, M. J. Black, and L. Sigal. Implicit probabilistic models of human motion for synthesis and tracking. In *Computer Vision-ECCV 2002*, pages 784–800. Springer, 2002.

[17] C. Wakim, S. Capperon, and J. Oksman. A markovian model of pedestrian behavior. In *Systems, Man and Cybernetics, 2004 IEEE International Conference on*, volume 4, pages 4028–4033 vol.4, Oct 2004.

[18] B. Ziebart, N. Ratliff, G. Gallagher, C. Mertz, K. Peterson, J. Bagnell, M. Hebert, A. Dey, and S. Srinivasa. Planning-based prediction for pedestrians. In *Intelligent Robots and Systems, 2009. IROS 2009. IEEE/RSJ International Conference on*, pages 3931–3936, Oct 2009.